AUV-CSEM: An Improvement in the Efficiency of Multi-sensor Mapping of Seafloor Massive Sulfide (SMS) Deposits with an AUV

Steve Bloomer
Ocean Floor Geophysics
Burnaby, BC, Canada
steve.bloomer@oceanfloorgeophysics.com

Matthew Kowalczyk
Ocean Floor Geophysics
Burnaby, BC, Canada
matthew.kowalczyk@oceanfloorgeophysics.com

Peter Kowalczyk
Ocean Floor Geophysics
Burnaby, BC, Canada
peter.kowalczyk@oceanfloorgeophysics.com

Steven Constable
Scripps Institution of
Oceanography
University of California, San
Diego
La Jolla, CA, USA
sconstable@ucsd.edu

Eldad Haber
Department of Earth, Ocean and
Atmospheric Sciences
University of British Columbia
Vancouver, BC, Canada
eldad@compgeoinc.com

Toru Kasuga
Fukada Salvage and Marine
Works Co. Ltd.
Tokyo, Japan
kasuga.toru@fukasal.co.jp

Abstract— **Seafloor massive sulfide (SMS) deposits are of interest because of their potential as copper and gold orebodies. This mineralization is often highly conductive, and consequently, electromagnetic mapping of these deposits for ranking of drilling targets often follows autonomous underwater vehicle (AUV) surveys that include multibeam bathymetry, side scan sonar, and chemical sensor data collection. This paper describes the results of two engineering tests to enable the simultaneous collection of standard payload AUV data with electromagnetic data for rapid determination of drilling targets. The resulting system is shown to be an efficient and cost-effective method for concurrent high-resolution multisensor and electromagnetic mapping in an SMS environment.**

Keywords—autonomous underwater vehicle, submarine massive sulfides, controlled source electromagnetic, self-potential, multibeam, bathymetry, 3-D inversion, 3-D visualization

I. INTRODUCTION

Seafloor massive sulfide (SMS) deposits found near seafloor hydrothermal venting sites are of economic interest because they contain metals such as gold and copper at high enough grades to be potential orebodies. These deposits were first discovered in 1980 [1]. Serious exploration for these deposits has been ongoing in the last decade because of their potential to be highly profitable in the future and as a strategic requirement of many nations to secure stable supplies of metals for their industrial base.

Typically, the search for new vent fields starts with regional mapping consisting of shipborne bathymetry to identify appropriate seafloor morphological features such as calderas. Towed ocean chemistry surveys with side-scan sonar are then done to detect plumes that identify locations for follow up high-resolution surveys. These detailed surveys of SMS fields are typically done with AUVs using multibeam sonar (MBES), side-scan sonar (SSS), sub-bottom profilers (SBP), water chemistry sensors, and magnetometers.

In addition to the sensors listed above, electromagnetic (EM) methods are also useful for mapping SMS deposits. EM methods can map the subsurface distribution of these deposits in detail because SMS mineralization containing copper or gold is often highly conductive. This is a strong argument for the use of EM in an SMS exploration program because EM can identify the SMS deposits most likely to contain economic mineralization and, consequently, allows a rapid ranking of targets for drilling. However, EM surveying has been typically done separately from the AUV component of the follow up high-resolution surveys.

This paper presents the results of two engineering tests mounting electrodes to an AUV to enable simultaneous collection of data from a standard AUV payload and EM systems. These tests were conducted by OFG, Fukada Salvage and Marine Works (Fukada), and the Scripps Institution of Oceanography (Scripps). The resulting AUV-mounted controlled source electromagnetic system (AUV-CSEM) has successfully demonstrated that it can provide an efficient and cost-effective method to do subsea EM in the SMS exploration environment. AUV-CSEM systematically applied in conjunction with data collected with the other AUV sensors provides opportunities for very efficient exploration, leading rapidly to the discovery of buried and inactive SMS deposits, and the ranking of drill targets.

II. MARINE EM SURVEYS

EM surveying is useful for ranking potential drilling targets in SMS exploration. Consequently, there has been an

ongoing development of marine EM systems for this purpose. In 2008, Ocean Floor Geophysics Inc. (OFG) developed and patented the first EM system to successfully map the limits of conductive near-surface mineralization in a survey of an SMS deposit at Solwera1 [2]. Since then, towed coincident loop time domain systems have been developed. The Waseda University system [3] in offshore tests have detected mineralization buried at 30 m. The Golden Eye system [4] has detected both conductivity and chargeability anomalies over SMS fields along the Central Indian Ridge. Clear anomalies have been detected over sulfide mineralization at the TAG field on the mid-Atlantic ridge using a deep-tow controlled source electromagnetic system (CSEM)[5].

In addition to EM methods using an active source, self-potential measurements can be used in the marine environment for the study of SMS deposits. In early surveys on land, self-potential measurements over metal ore bodies were observed to produce negative potential anomalies, with [6] presenting a classic model that explains this phenomena as the result of oxidation-reduction gradients across the ore body. In the marine environment, SP measurements were first documented in [7]. Likely the first successful application of marine SP in studies of SMS deposits was with an electrode array connected to the submersible Cyana in a survey of a seamount near the axis of the East Pacific rise [8]. A similar procedure was used in [9] in a submersible Alvin survey of the TAG hydrothermal mound. More recent SP studies using a towed array showed that SP was critical in the detection of potential SMS targets in the northern equatorial zone of the Mid-Atlantic Ridge [10] and that SP methods could be used to detect buried SMS deposits in a survey of Izena hole in the Okinawa trough [11].

Over the last four years, using a controlled electrical source and an array of CSEM receivers described in [12], OFG has partnered with Fukada and Scripps to successfully map methane hydrate deposits to several hundreds of meters below the seafloor. These methane hydrate deposits are resistive targets and the extension of this CSEM technology to map conductive SMS deposits to a comparable range of depths below the seafloor would be valuable.

However, towed CSEM systems consist of a long array of electrical transmitters and receivers. Therefore, a large ship is required to tow the system. For surveys with high spatial resolution with tight line spacing, slow towing speeds and time-consuming turns (up to 4 hours) are required. Additionally, it would be difficult to tow the system at a constant low altitude that was used in mapping hydrate deposits in the rugged terrain associated with hydrothermal vents.

To mitigate these problems, reduce costs on ship and crew to deploy the system, and to enable the simultaneous collection of high-resolution complementary data (MBES bathymetry, SSS, SBP, ocean chemistry, magnetometry), an AUV-CSEM concept was developed to (1) use battery powered transmitters placed on the seafloor to generate electrical fields that interact with the subsurface geology; (2) integrate the EM receiver electrodes into the Fukada AUV "Deep1" to measure the resulting electric fields; and (3)

eventually use these E-field measurements to generate 3-D subsurface conductivity distributions over the survey area. This paper will summarize the highlights of two AUV-CSEM engineering tests performed in 2015 and 2016 by OFG, Fukada, and Scripps to resolve technical uncertainties and advance the use of CSEM technology with a survey AUV as a platform.

III. RESULTS OF THE FIRST ENGINEERING TEST

The first engineering tests involved measuring the ambient electric field on the CSEM electrodes mounted to an AUV without any transmitted electrical (E-) field during the test. EM modelling prior to the AUV tests demonstrated that significant EM anomalies above background could be detected using a standard towed CSEM system. The E-field noise levels generated by an AUV were not known prior to the test, but it was thought that the noise levels would be sufficiently low to enable useful CSEM data, while causing only minor loss of AUV vehicle performance.

This test was performed in 2015 in Nago Bay, Okinawa, Japan in approximately 300 m of water. CSEM electrodes and an underwater data logger were contributed by Scripps. Fukada provided ship time and the AUV and modified the vehicle for mounting the electrodes. OFG designed and fabricated the mounting apparatus for the electrodes. OFG and Fukada assembled the apparatus and electrodes on the AUV. Two pairs of electrodes were mounted perpendicular to the main axis of the AUV, with one pair mid AUV and one pair closer to the vehicle propeller (Fig. 1). The subsea data logger was secured in the main flooded section of the AUV to record the ambient electric fields.

An experiment was designed to study how the ambient noise levels on the E-field measuring electrodes changed while varying operational parameters. A series of short survey loops were run, while turning off the payload devices (sonars, magnetometers, and chemical sensors) one by one and varying the heading of the vehicle. Later, the speed of the vehicle was varied by changing the propeller rotation rate while running a series of short lines. Finally, a short, but typical, sonar multibeam survey was run to determine the effect of the drag of the electrodes on the AUV speed over ground and on vehicle energy consumption.

Fig. 1: The first (2015) test set up with a pair of electrodes mounted on top of Fukada's Deep1 AUV.

After the test, the data were divided into subsets for each set of operational parameters. Spectra were then generated on these subsets, and the time series data and the spectra were analyzed. Three major observations were made:

1) The principal source of the noise was related to the thruster system and the payload devices had little effect on the noise level on the electrodes (Fig. 2).

2) The noise level varied with the heading of the vehicle, the orientation of the electrodes, and the position of the electrodes with respect to the thruster.

3) The speed tests showed that the noise on the electrodes had a red spectrum, with noise power decreasing with frequency with a series of narrow spectral peaks superimposed on that spectrum. These narrow peaks correspond to the rotation rate of the propeller of the AUV and its harmonics (Fig. 3), consistent with the hypothesis that the thruster system is the principal source of noise.

These observations were very encouraging. Since the noise added by the payload devices was minor, CSEM and standard payload surveying can be run simultaneously during a survey, increasing survey productivity and providing more data to aid geological interpretation for determining drill targets. As well, despite the presence of narrow, propeller related, peaks in the noise spectrum, there are bands of reduced noise between the peaks that can be matched with peaks in the transmitted electric field spectra to produce bands in the electric field spectra with high signal to noise ratios. This can be easily done by adjusting the rotation rate of the AUV propeller relative to the known source waveform spectral peaks.

Finally, the AUV speed for the small multibeam survey was reduced from an expected 1.5 m/s to 1.1 m/s due to the increased drag caused by the electrodes. Power consumption was approximately 0.8 kWh/hr of dive time, which is slightly more than a typical 0.7 kWh/hr for a Deep 1 survey. At these rates of AUV speed and battery consumption, 50 lines kilometers would be achievable in a 24-hour dive plus battery charge cycle, which would be better than the 40-line kms/day achieved with a ship towed system. Despite of the negative effects of drag caused by the electrodes, the logistics of the AUV system are still more efficient than a towed system, because of the absence of large turns. Additionally, payload data can be collected without affecting the electric field data, and navigation of the AUV over the seafloor is improved.

IV.   SEAFLOOR TRANSMITTER TEST

The results of the first set of tests indicated a strong possibility that a AUV-CSEM survey system would be successful. The last remaining uncertainty was the range from the AUV to a Scripps ocean bottom EM transmitter in which high quality E-field data could be collected. Forward modelling results suggested that to a range of 350 m from the transmitters, operating with a standard transmitted current, useful E-field data could be collected in a conductive region. It was also thought that the bands of low spectral noise were sufficiently wide that two or more transmitters, transmitting signals with different fundamental frequencies, could be operated simultaneously and that their signals could be separated.

For the transmitter test in 2016, an AUV electrode configuration like the 2015 test was used, with a pair of addition vertical electrodes added mid-AUV. The Scripps seafloor transmitters were battery powered and transmit a programmable binary waveform into an orthogonal pair of 10 m antennas (Fig. 4). The battery life of each transmitter with a standard transmit current was approximately 12 hours. The transmitter assemblies, which included flotation and a
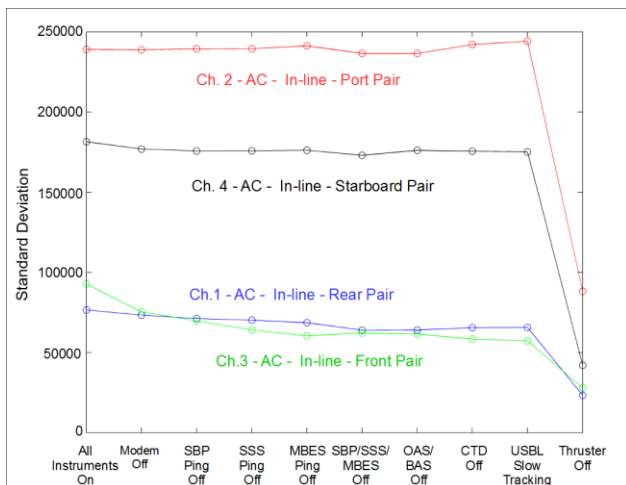

Fig. 2: The noise levels on the AC channels as the payload equipment was successively turned off, with the actions indicated on the bottom axis. The noise level with all the equipment on is only slightly higher than most of the equipment turned off. Turning the vehicle motor off was the only action that substantially decreased the noise level, indicating the primary noise source was related to the thruster.
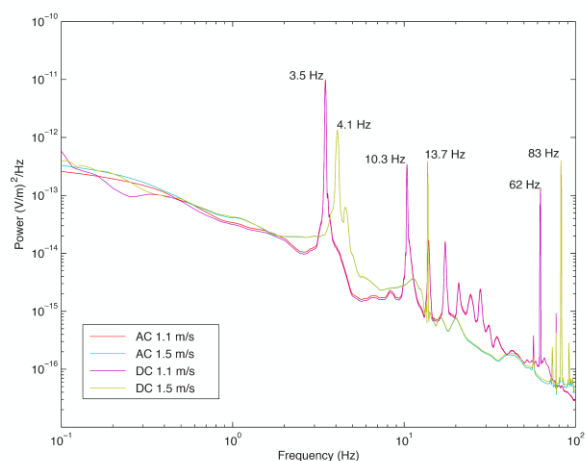

Fig. 3: Noise spectra run at two speeds showing shift in spectral peaks. The spectral peaks appear to be related to the frequency of the vehicle propeller. A 1.1 m/s AUV speed was achieved with a propeller rate of 201 RPM (~3.35 Hz) while the 1.5 m/s AUV speed was achieved with 264 RPM (~4.4 Hz).
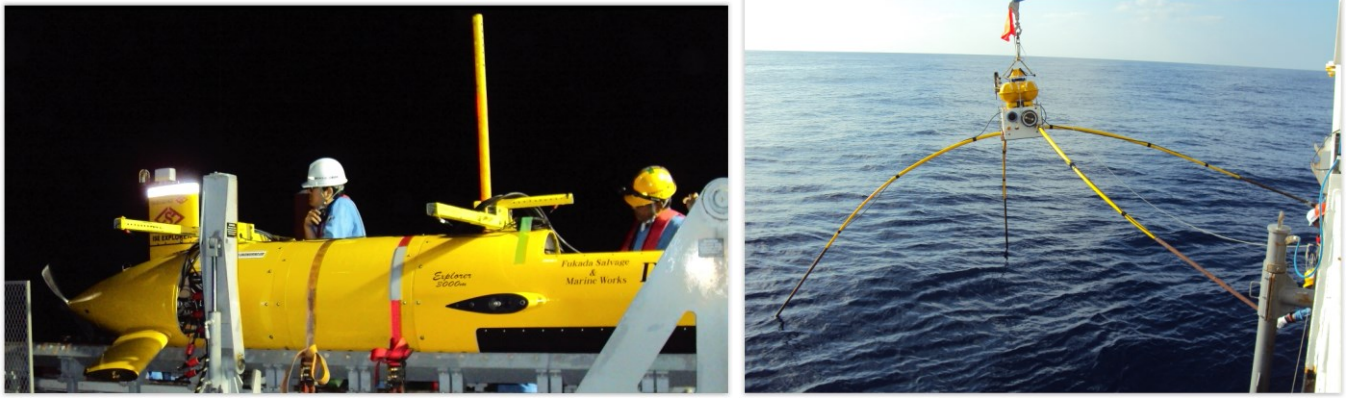
Fig. 4: AUV CSEM survey, Sea of Japan Nov 2016. Left, AUV with electric dipole mounts on AUV, including a vertical pair of electrodes. Right, Scripps DUESI seafloor transmitter being deployed.

weighted platform, were equipped with an USBL positioning beacon to monitor its descent to the seafloor and to determine its final resting position and with an acoustic release to enable recovery at the end of the survey

The survey took place offshore Japan in the Iheya Ridge area of the Okinawa Trough at a water depth of approximately 1500m. The general area of this survey is known for active hydrothermal venting and SMS deposits [13] [14]. A previous survey at the site indicated there were hydrothermal vent chimneys in the planned survey area. The planned survey consisted of three roughly SW-NE 1 km lines space 100 metres apart, with one line along the axis of a line of chimneys, and a perpendicular set of 1 km intersecting the three other lines in the middle of the survey grid and running through more chimneys.

The planned locations of the two transmitters were approximately at opposite corners of the 200m square defined by the intersection of the survey lines. A third transmitter was deployed prior to the survey to determine the drift offset of the transmitter platform due to strong ocean currents. This drift offset enabled the two transmitters for the test to be located within 100m of their planned locations, resulting in the central region of the survey area to fall within the expected range of the transmitters. The two transmitters broadcasted 20 A at a frequency of 2 and 2.5 Hz and harmonics, with the transmission polarities alternated every 30 s.

The survey grid was run three times at a nominal altitude of 70m above the seafloor. The transmitter on times were synchronized with the AUV mission to optimize transmitter battery consumption and to attempt to create a survey test with one circuit of the survey grid run only the first transmitter on, once with both transmitters on, and once with only the second transmitter on. This synchronization of current transmission and repeated survey circuits was achieved, with electrical field data collected on all three runs along with the full suite of AUV payload data: multibeam bathymetry, sidescan sonar backscatter, subbottom profiler, OFG Self-Compensating Magnetometer (SCM) system, optical backscatter (turbidity), temperature, and ocean chemistry (pH and ORP - oxidation reduction potential) data.

Final navigation for the survey was produced by shifting

the navigation from the inertial navigation system of the AUV, which drifts as a function of distance travelled, to the USBL navigation on a line by line basis using a least squares minimization to calculate shifts in eastings and northings. By picking the positions to the top of the numerous chimneys, a 5m accuracy between positions in the three circuits was established. Although the positional accuracy could be improved by matching the bathymetric features between circuits, the navigational accuracy is sufficient to produce a consistent navigational basis between the three circuits run during the survey to evaluate the utility of an AUV platform for CSEM surveys, and for the EM analysis described below. For this assessment, the success of the test was gauged by: (1) how well the measured CSEM response of the massive sulfide system at this site coincided with a field of SMS mounds and active hydrothermal chimneys (Fig. 5) and (2) how consistent the results of the CSEM response were from circuit to circuit as the transmitters were turned on and off.
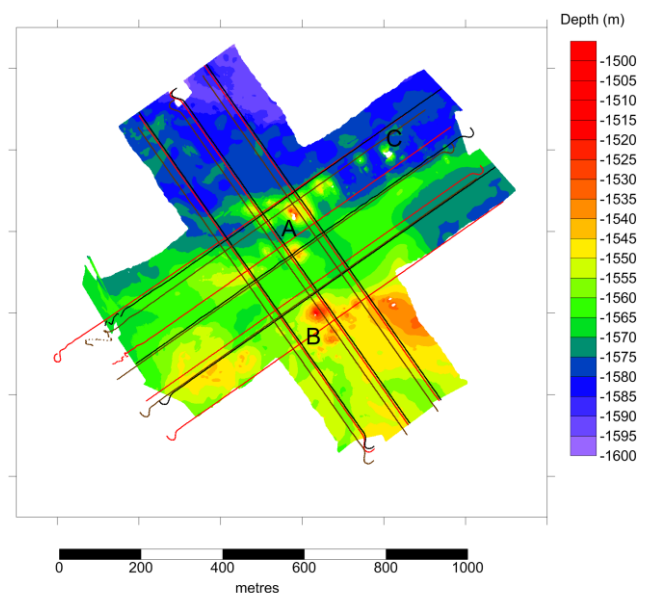

Fig. 5: Bathymetry map of the test area derived from circuit 1 multibeam bathymetry data. AUV tracks from circuit 1 (black), circuit 2 (brown), and circuit 3 (red) are shown. Labels A-C show area of anomalous self-potential.

V. SEAFLOOR TRANSMITTER TEST RESULTS

The test results were very positive. The SP and CSEM results presented here are summarized in [15]. We successfully measured the CSEM response of a hydrothermal chimney system with a strong anomaly over chimneys presumed to contain massive sulfides. A comparison of the DC electric field data from three sets of traverses showed a strong consistency (Fig. 6) and demonstrates that we can operate at least two transmitters concurrently using separated fundamental frequencies. The data over the entire survey area was of high quality, with an estimated transmitter range estimated to be at least 400m.

We also successfully operated all the AUV payload systems while making these CSEM measurements. This enabled the comparison of CSEM and groundtruth datasets by using 3-D visualization tools (Fig. 7). Fig. 8 shows a single frequency 1-D apparent conductivity map derived from the electric field data recorded during one of the circuits of the test. The two order of magnitude range of the conductivities is capable of distinguishing conductive bodies (~10 S/m) from resistive geology (~0.1 S/m). Comparison of this figure to the bathymetry (Fig. 5) shows that high apparent conductivities for this frequency correspond to the bathymetric highs at B.

The apparent conductivity anomalies are interpreted to represent massive sulfides. The southern conductivity high corresponds to a series of mounds. The electric field data is also more spatially consistent than the oxidation-reduction potential data measured in the water column, suggesting that strong currents and/or episodic venting effect the distribution of the chemical plumes, and the consistent conductivity anomalies are thus related to the local geology (Fig. 9).

Additionally, Fig. 8 is the result from a single frequency of a multi-transmitter, multi-frequency CSEM survey. The CSEM data were collected at multiple frequency bands with high signal to noise ratios between 2 to 20 Hz, providing a multi-frequency data set amenable to 3D inversion to map out the burial depth and limits of the conductive zones. A preliminary inversion of the CSEM data was performed using the total electric field data at multiple frequencies, producing a subsurface 3-D conductivity model shown in Fig. 7. The principal conductive body is centered beneath the large mounds in the southern section in the survey area and extends to depth. However, the sensitivities used in the inversion were suboptimal, with higher sensitivities towards the transmitter and the seafloor. It is suspected that abnormal higher conductivities have been concentrated close to the transmitter locations as a result. This is observed in high conductivity zones in the inversion model near the northwest transmitter. The extension to depth of the main conductor in a region of lower sensitivity suggests this conductor is real.

In addition to the apparent conductivity maps generated from this data, mounting the E-field sensors on the AUV allows a highly sensitive self potential (SP) measurement to be made. An Occam inversion was used to integrate DC electric fields with irregular data spacing to SP data on a uniform grid, using the approach of [16]. Here, the results (Fig. 10) show a much stronger SP anomaly over the more northern set of mounds (point A). The cause of the SP anomaly is uncertain: it may due to mineralization, or hydrothermal venting, or both. Given that the venting and SMS deposits are related, it still is a useful measurement in a suite of data for characterizing potential drilling targets.

VI. CONCLUSIONS

This paper has presented the results of two successful tests that demonstrate the capability of mounting electrodes to an AUV for EM prospecting of geological targets. The example pilot study showed its capability to accurately map conductive SMS targets, but would even be more effective mapping resistive targets, such as gas hydrate deposits, where transmitter ranges would even be longer due to less signal attenuation. The CSEM-AUV system presented here is more
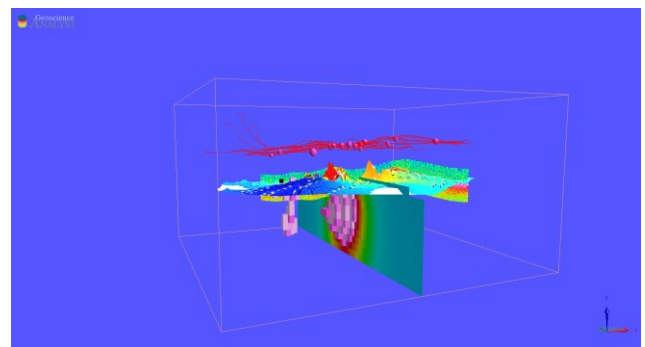
Fig. 7: 3-D data model of the AUV-CSEM data. On the top layer are the AUV tracks and the locations of the ORP minima (pink spheres). The SP inversion result from Fig. 10 is painted on the multibeam bathymetry (vertical exaggeration 2x). Beneath the seafloor surface, a subbottom profile is displayed. The inverted conductivity model derived from the CSEM data is displayed as both a vertical slice through the model and an isosurface. The volume is approximately 1100m x 1200m x 250m.
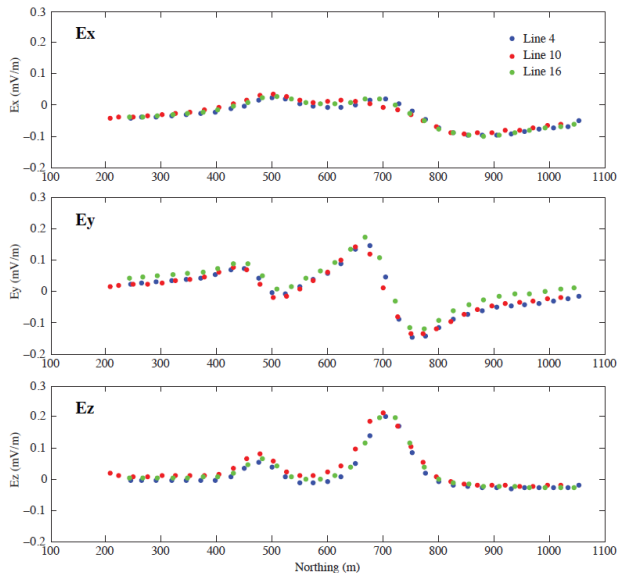

Fig. 6: 30 second averages of the electric field data, after levelling, for the eastern most lines of the southeast-northwest lines of the three repeated circuits.
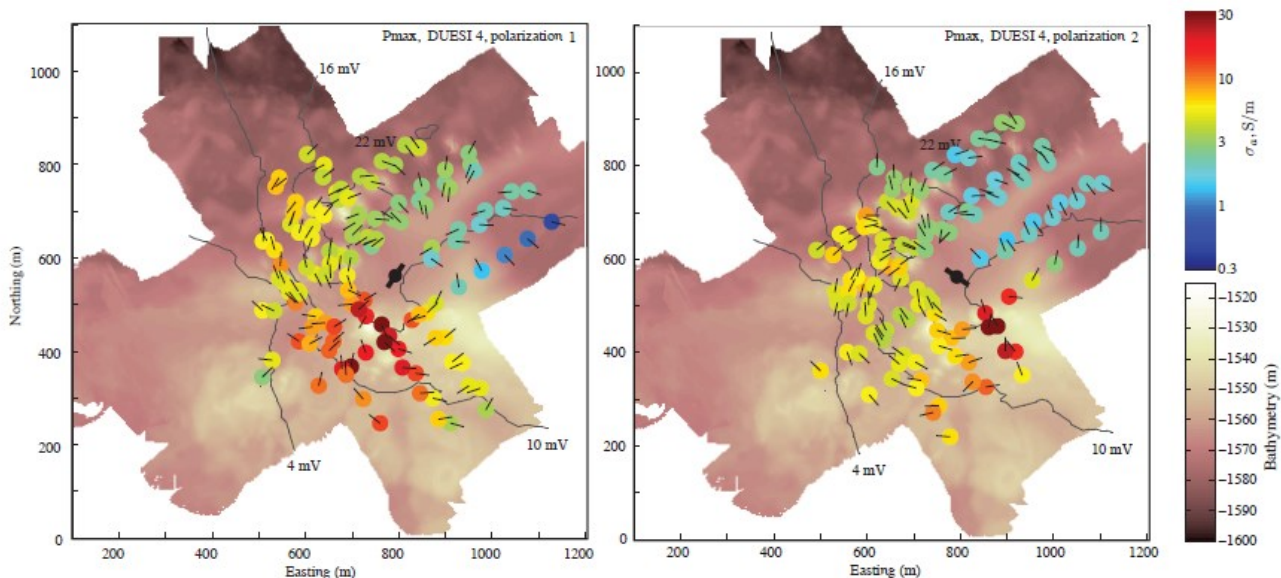
Fig. 8: Apparent conductivity (colored disks – log10 scale) overlain on bathymetry for two polarizations of CSEM transmission from a deployed transmitter (center black symbol). For this example, the transmission frequency is14 Hz, and the black lines show the directions of the polarization ellipse maxima recorded by the AUV.

efficient than a towed system and has the added benefit of a suite of complementary instrumentation to aid interpretation.

These tests have also indicated the necessary improvements required for future surveys. For the initial tests presented here, the electrode mounting hardware was simple with the purpose of extending the electrodes away from electrical interference from the vehicle. This resulted in drag on the vehicle, limiting the speed of the AUV and increasing the battery consumption. For future measurements, the dipoles will be streamlined to reduce drag, and increase the mapping

productivity of the vehicle. Transmitter design will be improved, especially increasing the output current to increase transmitter range and acoustic control of the on/off switching of the transmitter to conserve battery power and enable an efficient survey to be run by enabling the AUV to pass from the range of one transmitter to another.

REFERENCES

[1] Speiss, F.N., Macdonald, K.C., Atwater, T., Ballard, R., Carranza, A., Cordoba, D., Cox, C., Diaz Garcia, V.M., Francheteau, J., Guerrero, J., Hawkins, J., Haymon, R., Hessler, R., Juteau, T., Kastner, M., Larson, R., Luyendyk, B., Macdougall, J.D., Miller, S., Normark, W., Orcutt, J., and Rangin, C., "East Pacific Rise: hot springs and geophysical
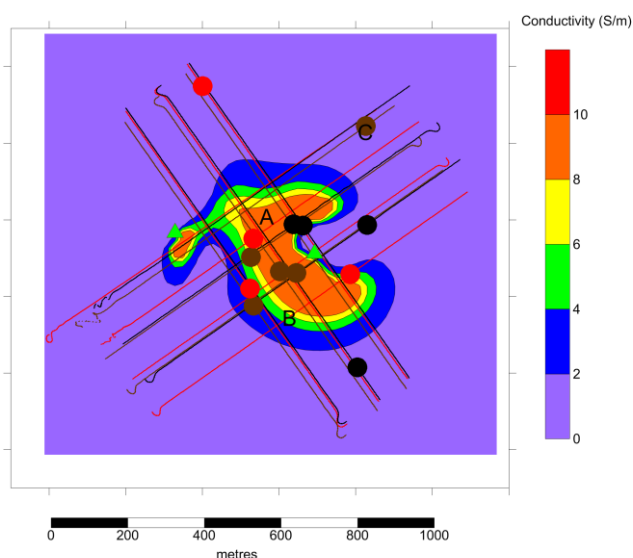
Fig. 9: Plan map view of a 3D model of the inverted CSEM conductivity at a depth of 1632 mbsf. The 2 green triangles are the transmitter positions, while the locations of the ORP minima for the entire survey are plotted as black circles for circuit 1, brown circles for circuit2, and red circles for circuit 3.
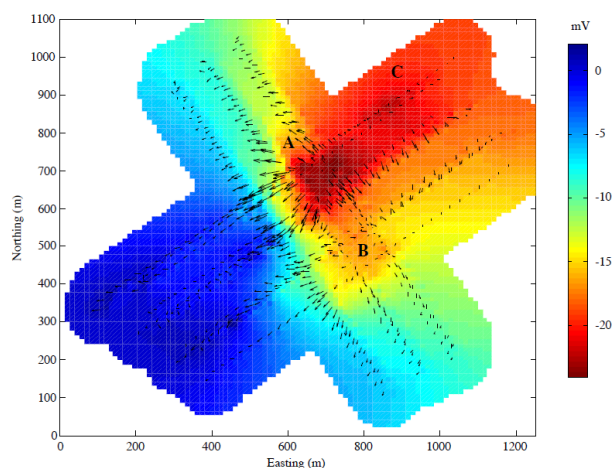

Fig. 10: Self potential derived from Ex and Ey data shown in Fig. 6 by Occam's inversion. Arrows show the directions of the potential differences as measured by the AUV CSEM system, scaled by amplitude.

experiments", Science, vol. 207, pp.1421-33, 1980.

[2] Kowalczyk, P., "Geophysical prelude to first exploitation of submarine massive sulphides", First Break, vol. 26 Nov 2008.

[3] Nakayama, K. and Saito, A., "The seabed TDEM towed by ROV for the ocean bottom hydrothermal deposits", EAGE First Conference on Geophysics for Mineral Exploration and Mining - Near Surface Geoscience, Barcelona, September 2016.

[4] Schwalenberg, K., Muller, H., and Engels, M. "Seafloor massive sulfide exploration – A new field of activity for marine electromagnetics", EAGE/DGG Workshop on Deep Mineral Exploration, Munster, March 2016.

[5] Murton et al., Cruise Report JC138, National Oceanography Centre, Southampton UK, 2017.

[6] Sato, M., & H.M. Mooney, "The electrochemical mechanism of sulphide self-potentials", Geophysics, vol. 3, pp. 226–249, 1960.

[7] Corwin, R., "Offshore use of the self-potential method, Geophysical Prospecting", vol. 24, pp. 79–90, 1976.

[8] Francis, T.J.G., "Resistivity measurements of an ocean floor sulphide mineral deposit from the submersible Cyana", Mar. Geophys. Res., vol. 7, pp. 419–437, 1985.

[9] Von Herzen, R.P., J. Kirklin, & K. Becker, "Geoelectrical measurements at the TAG hydrothermal mound", Geophysical Research Letters 23, pp. 3451–3454, 1996.

[10] Cherkashev, G.A., V.N. Ivanov, V.I. Beltenev, L.I. Lazareva, I.I. Rozhdestvenskaya, M.L. Samovarov, I.M.Poroshina, M.B. Sergeev, T.V. Stepanova, I.G. Dobretsova, & V.Yu. Kuznetsov, "Massive sulfide ores of the northern equatorial Mid-Atlantic Ridge", Oceanology , vol. 53, pp. 607–619, 2013.

[11] Kawada, Y. and T. Kasaya, "Marine self-potential survey for exploring seafloor hydrothermal ore deposits", Scientific Reports, vol. 7, doi 10.1038/s41598-017-13920-0, 2017.

[12] Constable, S., P. K. Kannberg, & K. Weitemeyer, "Vulcan: A deeptowed CSEM receiver", Geochemistry, Geophysics, Geosystems, vol. 17, pp. 1042–1064, 2016.

[13] Glasby, G.P., Notsu, K., "Submarine hydrothermal mineralization in the Okinawa Trough, SW of Japan: an overview", Ore Geology Reviews, vol. 23, pp. 299-339, 2003.

[14] Yeats, C.J., S.P. Hollis, A. Halfpenny, J.-C. Corona, C. LaFlamme, G. Southam, M. Fiorentini, R.J. Herrington, and J. Spratt, "Actively forming Kuroko-type volcanic-hosted massive sulfide (VHMS) mineralization at Iheya North, Okinawa Trough, Japan", Ore Geology Reviews, vol. 84, pp. 20–41, 2017.

[15] Constable, S., Kowalczyk, P., and Bloomer, S., "Measuring Marine Self Potential using an Autonomous Underwater Vehicle", submitted to Geophysical Journal International, 2017.

[16] Constable, S.C., Parker, R.L., & Constable, C.G., "Occam's Inversion: a practical algorithm for generating smooth models from EM sounding data", Geophysics, vol. 52, pp. 289–300, 1987.